arXiv:1508.04878v1 [cond-mat.quant-gas] 20 Aug 2015

All-optical control of superradiance and matter waves using a dispersive cavity

Shih-Wei Su,[1] Zhen-Kai Lu,[2] Nina Rohringer,[3,4,5] Shih-Chuan Gou,[1] and Wen-Te Liao[3,4,5,6,*]

[1]*Department of Physics and Graduate Institute of Photonics,*
National Changhua University of Education, Changhua 50058 Taiwan
[2]*Max Planck Institute for Quantum Optics, D-85748 Garching, Germany*
[3]*Max Planck Institute for the Structure and Dynamics of Matter, 22761 Hamburg, Germany*
[4]*Max Planck Institute for the Physics of Complex Systems, 01187 Dresden, Germany*
[5]*Center for Free-Electron Laser Science, 22761 Hamburg, Germany*
[6]*Department of Physics, National Central University, 32001 Taoyuan City, Taiwan*

(Dated: Version of July 22, 2017.)

Cavity quantum electrodynamics (CQED) [1] plays an elegant role of studying strong coupling between light and matter. However, a non-mechanical, direct and dynamical control of the used mirrors is still unavailable. Here we theoretically investigate a novel type of dynamically controllable cavity composed of two atomic mirrors. Based on the electromagnetically induced transparency (EIT) [2, 3], the reflectance of atomic mirror is highly controllable through its dispersive properties by varying the intensity of applied coupling fields or the optical depth of atomic media. To demonstrate the uniqueness of the present cavity, we further show the possibility of manipulating vacuum-induced diffraction of a binary Bose-Einstein condensate (BEC) [4, 5] when loading it into a dispersive cavity and experiencing superradiant scatterings [6]. Our results may provide a novel all-optical element for atom optics [7] and shine new light on controlling light-matter interaction.

For decades, CQED has served as an elegant model for demonstrating atom-light interaction and fundamental principles of quantum mechanics [1]. In conjunction with the state-of-art experiments using ultracold atoms, CQED has been able to facilitate the realization of quantum metrology [8], quantum teleportation [9] and quantum memory storage [10], etc., experiments paving the way for the fulfillment of quantum technology. By its very nature, cavity is an indispensable ingredient to CQED, which reflects photons and has them interact with atoms in a confined space. However, conventional CQED systems consisting of reflecting mirrors limiting themselves from being networked at large scale. Here, we propose a novel cavity system where mechanical mirrors are replaced by atomic ensembles whose dispersion can be controlled by, e.g., EIT, and so we term it as dispersive cavity which offers unique controllability. Moreover, the separation between the atomic mirrors and their size can be much smaller than that of mechanical ones. Therefore, the cavity cooperativity is enhanced due to smaller cavity volume and it becomes more feasible to reach strong coupling regime and scalable for more demanding systems. Both advantages render fabricating a more functional matter-wave interferometry or atomic circuit possible. The dispersive cavity can also be integrated on atom chips [11] or used to study the cavity-mediated spin-orbit coupling in the ultracold atoms [12], bringing both the controllability and the tiny size into full play.

As depicted in Fig. 1 **a**, our dispersive cavity is composed of two remote collections of three-level-Λ type atoms. Based on EIT [13, 14], as illustrated in Fig. 1 **b** and **d**, each atomic medium constitutes a mirror when interacting with two counter-propagating coupling fields with Rabi frequencies $\Omega_c^{\pm}$ driving the $|2\rangle \leftrightarrow |3\rangle$ transition. Under the action of four-wave mixing [14], an incident probe field with Rabi frequency Ω^{+} driving the transition $|3\rangle \leftrightarrow |1\rangle$ will be reflected and generate a backward probe field with Rabi frequency Ω^{-} [13], and vise versa. For showing the controllability and novelty of the dispersive cavity, we consider an excited quasi one-dimensional binary BEC which transversely flies through it and emits photons [5]. As illustrated in Fig. 1 **c**, the binary BEC consists of atoms condensed in the ground state $|g\rangle$ and excited state $|e\rangle$. The photonic polarization and frequency of transition $|g\rangle \rightarrow |e\rangle$ match that of $|1\rangle \rightarrow |3\rangle$ of two atomic mirrors such that emitted photons with wavelength λ from BEC can be reflected by two side EIT media. The vacuum fluctuations [15] and the geometric shape of the BEC will speed up the decay and result in the emission of superradiance (SR) along BEC's long axis [6, 15, 16]. Therefore when the long axis of the loaded BEC is parallel to the cavity axis, the SR will circulate within a dispersive cavity and become subsequently releasable by switching off coupling fields. The coexistence of BEC and superradiant photons within a cavity enables the multiple scattering between them. This renders the generation of matter waves with high order harmonic of photon wave number possible, namely, the diffraction of matter waves [7]. Because the effect is triggered by vacuum fluctuations, we term it as vacuum induced diffraction of matter waves.

We first investigate the controllability of the novel cavity and calculate the reflectance of an EIT mirror by numerically solving the optical-Bloch equations [14, 17]

$$\partial_t\hat{\rho} = \frac{1}{i\hbar}\left[\hat{H},\hat{\rho}\right] + \hat{\rho}_{dec}, \tag{1}$$

$$\left(\frac{1}{c}\partial_t \pm \partial_z\right)\Omega^{\pm} = i\eta_{EIT}\rho_{31}^{\pm}, \tag{2}$$

where $\hat{\rho}$ is the density matrix for the state vector $\sum_{i=1}^{3} B_i|i\rangle$ of the three-level atom in the Fig. 1 **a, b** and **d**. Also, $\hat{\rho}_{dec}$ describes the spontaneous decay of the excited state $|3\rangle$ characterized by rate Γ. $\hat{H}$ is the Hamiltonian for the interaction between atomic mirrors and counter-propagating fields (see Methods). Moreover, $\eta_{EIT} = \Gamma d^{opt}/2L$ with d^{opt} and L being the optical depth and the length of the medium, respectively.

---

[*] wenteliao@cc.ncu.edu.tw

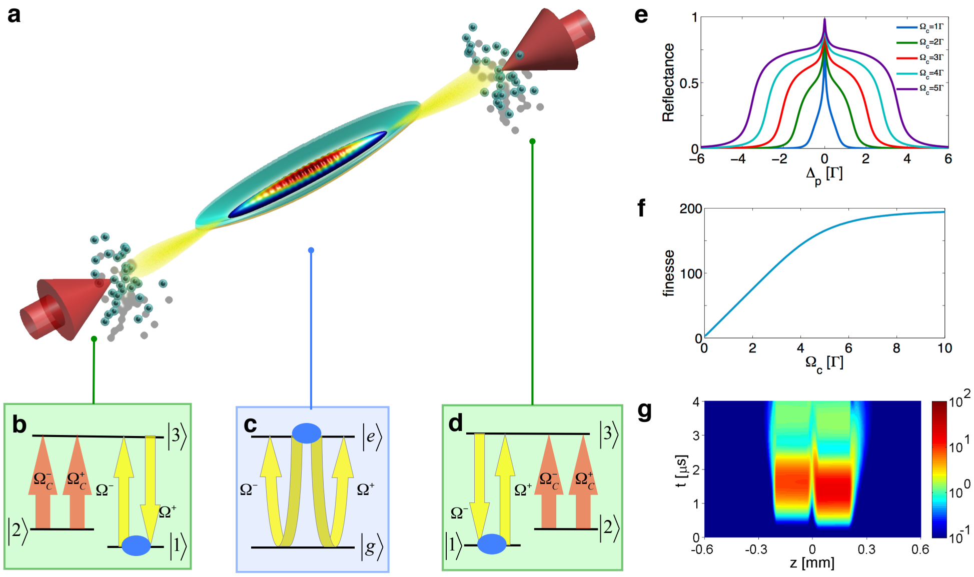

FIG. 1. **Schematic plot of a dispersive cavity.** **a**, a binary BEC sandwiched by two three-level EIT media, where the former is initially in the state $|e\rangle$ and the latters are in state $|1\rangle$. The red arrows represent two counter-propagating coupling fields driving the transition $|2\rangle \to |3\rangle$ as shown in **b** and **d**. The quantum fluctuations of binary BEC spontaneously generate the forward and backward SR fields $\Omega^\pm$ (yellow) as shown in **c**, which connect the EIT transition from $|1\rangle \to |3\rangle$. The composition of three-level atoms and coupling fields acts as a dispersive cavity, which reflects resonant yellow photons. The controllable reflectance of a dispersive mirror and the enhancement of cavity finesse are shown in **e** and **f**, respectively. **g**, the coherently trapped superradiant field $[|\Omega^+(t,z)|^2 + |\Omega^-(t,z)|^2]/\Gamma^2$ is shown where EIT mirrors are located in the regions $|z| > 0.2$ mm.

The resultant dispersive cavity has only one reflecting band whose width is associated to the EIT transparency window $\Delta\omega_{EIT} = \Omega_c^2/\left(\Gamma\sqrt{d^{opt}}\right)$ which is highly tunable by either varying the optical depth or the coupling fields. As shown in Fig. 1 **e**, at various detuning and a fixed optical depth $d^{opt} = 500$, the reflectance approaches unity when the fields $\Omega^\pm$ are resonant and the width can be controlled by varying the intensity of the coupling fields. To gain more insight into the dispersive cavity, we invoke the effective cavity finesse $f(\Delta_p) = \frac{\pi}{1-R(\Delta_p)}$ where $R(\Delta_p)$ is the reflectance as a function of the detuning Δ_p of fields $\Omega^\pm$ [18]. The cavity finesse is plotted in Fig. 1 **f**, which demonstrates that the cavity finesse can be controlled by tuning the EIT transparency window [2, 3].

We are ready to show the cavity effect on the BEC dynamics by numerically integrating equations (1) and (2) together with the coupled Gross-Pitaevskii equation which reads [19, 20] (see methods)

$$i\hbar\partial_t\begin{pmatrix}\psi_g\\ \psi_e\end{pmatrix} = \begin{pmatrix}H_{sp}+H_{int}^g & H_{atom-light}\\ H_{atom-light}^* & H_{sp}+H_{int}^e-\frac{i\Gamma}{2}\end{pmatrix}\begin{pmatrix}\psi_g\\ \psi_e\end{pmatrix}, \qquad (3)$$

where $\psi_{g,e}$ are the wave functions of the binary BEC, H_{sp} the single-particle Hamiltonian, $H_{int}^{g,e}$ the atom-atom interaction, $H_{atom-light}$ the atom-light interaction (see Methods), and Γ is the spontaneous decay rate of the excited level $|e\rangle$ introduced phenomenologically. To start up the superradiant process of the binary BEC in a cavity, the vacuum fluctuation is introduced by truncated Wigner method [21] (see methods). The dynamics of the generated SR fields is described by

$$\left(\frac{1}{c}\partial_t \pm \partial_z\right)\Omega^\pm = i\eta_{BEC}\sigma_{eg}^{(\pm1)}, \qquad (4)$$

where $\sigma_{eg}^{(\pm1)}$ is the coherence of the BEC associated with the plane-wave factor $e^{\pm ik_p z}$ (see Methods for details) and $\eta_{BEC} = 3\Gamma N_{BEC}\lambda^2/4\pi A$ with A being the transverse cross section of the condensate. In the following, we consider the EIT mirror of optical depth $d^{opt} = 500$ and coupling field of $\Omega_c = 2\Gamma$. A quasi one-dimentional BEC of ^{7}Li at $2S_{1/2}$ ($|g\rangle$) state can be prepared in a single beam dipole trap. An additional TEM$_{01}$-type laser mode beam is applied to cross the atomic ensemble [22]. The spatial intensity distribution of the cross beam allows to trap low density thermal clouds aside as the EIT mirrors while leaving the central BEC undisturbed. The ^{7}Li BEC can be coherently transferred to the excited $3P_{3/2}$ ($|e\rangle$) state by a π pulse. The narrow linewidth of $3P_{3/2}$ state, $\Gamma \sim 760$ kHz [23] offers a reasonable time scale for detection. Moreover, $d^{opt} = 1000$ has already been experimentally achieved in cold atom systems [24, 25]. As an example, with $N_{BEC} = 3 \times 10^5$ and $A = (\pi \times 3^2)\ \mu\text{m}^2$, Fig. 1 **g** depicts the intensity of the confined superradiance $|\Omega^+(t,z)|^2 + |\Omega^-(t,z)|^2$ in a dispersive cavity.

The three steps of vacuum induced diffraction of matter waves is shown in Fig. 2 **a**, namely, from top to bottom, creating BEC in state $|e\rangle$, loading BEC into a dispersive cavity and releasing BEC. The multiple-scattering between circulating SR fields and the BEC generates higher order harmonics of the matter wave. Theses high k_p modes can be clearly observed by time-of-flight (TOF) simulation with $N_{BEC} = 10^6$

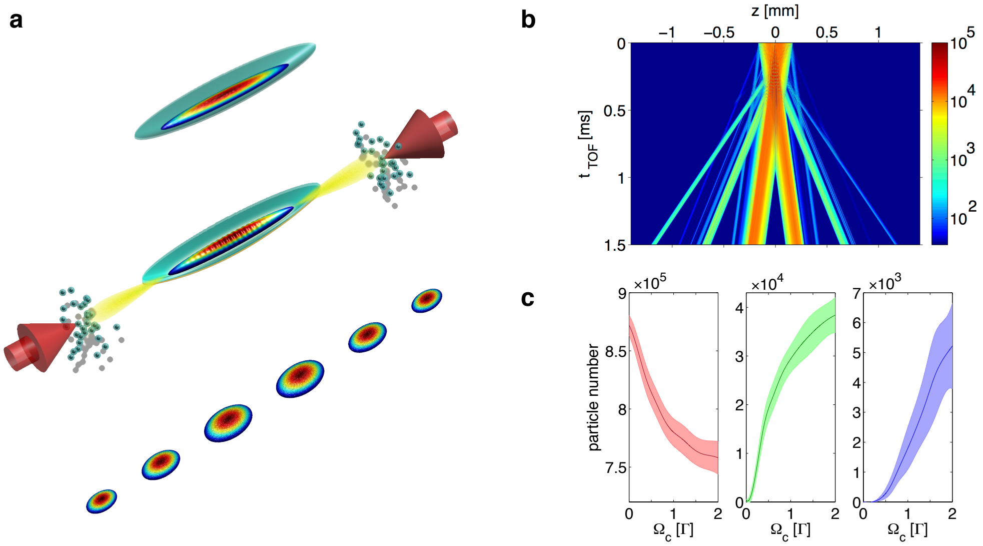

FIG. 2. **Controllable vacuum induced diffraction of matter waves using a dispersive cavity.** **a**, coherent matter waves initially prepared in its internal excited state are diffracted by three steps from top to bottom. The condensate is created in a harmonic trap (green surface) and flies through a dispersive cavity where odd multiple k_p modes of matter waves emerge. When switching off the trap, matter waves of different modes split due to the momentum kick from SR photons, namely, atomic diffraction. **b**, the BEC's time of flight dynamics. Six density bumps carrying momenta of $\pm k_p$, $\pm 3k_p$, and $\pm 5k_p$ can be clearly observed at the end of time. **c**, the coupling-field-strength-dependent mean particle number of different modes of diffracted BEC carrying $\pm k_p$ (red), $\pm 3k_p$ (green) and $\pm 5k_p$ (blue). All the data points are averaged over 1000 realizations, and the color filled regions illustrate the corresponding error bars.

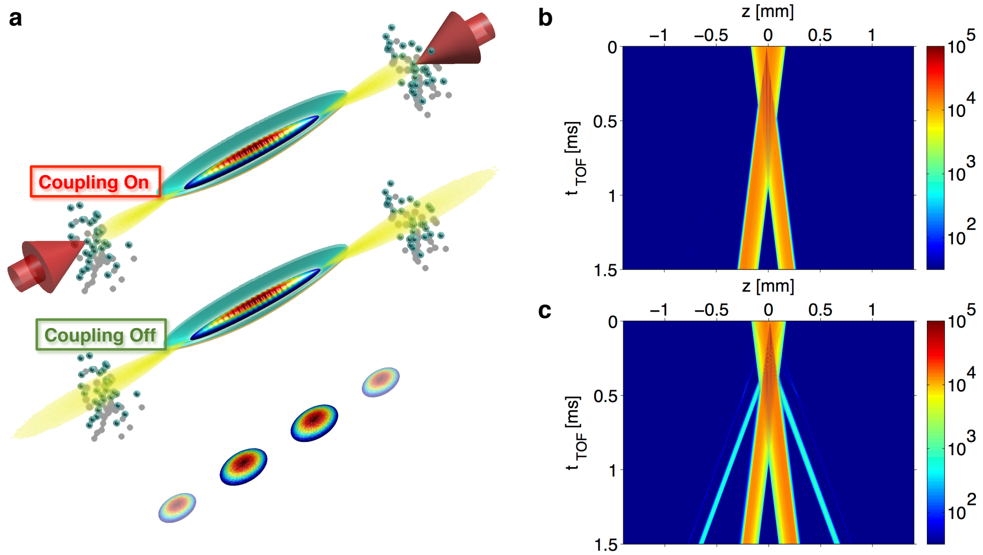

FIG. 3. **Dynamical control of vacuum induced diffraction of matter waves using a dispersive cavity.** **a**, when loading BEC into a dispersive cavity, atomic diffraction can be dynamically controlled by turning off the coupling field at different instance. The time of flight for that coupling field is off at **b** 0.02 μs and **c** 0.07 μs after loading BEC. The particle numbers on each mode of **b** and **c** are $(N_{\pm k_p}, N_{\pm 3k_p}, N_{\pm 5k_p})$ =$(8.6\times 10^5, 300, 0)$ and $(8.2\times 10^5, 1.6\times 10^4, 200)$, respectively.

as shown in Fig. 2 **b**. Especially at t_{TOF} = 1.5 ms there are six notable peaks corresponding to $-5k_p$, $-3k_p$, $-k_p$, k_p, $3k_p$ and $5k_p$ from left to right. To study the controllability of generating high-k_p modes, we tune the cavity finesse by varying the strength of coupling fields and perform 1000 independent realizations for statistics. As shown in Fig. 2 **c**, the population of $\pm k_p$ modes is gradually and coherently transferred to that of higher order harmonics while increasing Ω_c. The particle number of $\pm 3k_p$ and $\pm 5k_p$ modes are significantly generated when $\Omega_c \gtrsim 0.1\Gamma$ and 1Γ, respectively. This is in contrast to the situation without the dispersive cavity where only $\pm k_p$ modes and very small fraction of $\pm 3k_p$ modes are generated, namely, about a factor of 1000 enhancement by the cavity for $\pm 3k_p$ modes. Remarkably, $\pm 5k_p$ modes only emerge under the action of a dispersive cavity.

Figure 3 illustrates the possibility of dynamically manipulating atomic diffraction. In Fig. 3 **a** we demonstrate a protocol to suppress the generation of particular harmonic of k_p matter wave by switching off two coupling fields at some instance, which dynamically disables the dispersive cavity. We respectively turn off the coupling fields at 0.02 μs and 0.07 μs in Fig. 3 **b** and Fig. 3 **c** after BEC is loaded. Our TOF simulations show that $\pm 3k_p$ and $\pm 5k_p$ modes can be successfully suppressed by release SR photons at proper instances before corresponding multiple scattering happens.

In conclusion, the novel flexibility of a dispersive cavity may give the possibility of implementing more delicate manipulations of matter wave and becomes all-optical elements for atom optics. Additionally, an all-optical Q-switching superradiant source may result from combining our system with triggered superradiance [26]. Moreover, the recent advance on x-ray quantum optics [27, 28] also shows the potential of achieving atomic mirrors in x-ray domain [29]. Given the high, non-mechanical and dynamical controllability of the dispersive cavity , the present system provides a unique and novel stage of manipulating light-mater interaction.

METHODS

In the presence of the counter-propagating coupling and SR fields, the Hamiltonian of the EIT medium is $\hat{H} = \hat{H}_0 + \hat{H}_I$ where $\hat{H}_0 = \sum_j \hbar\omega_j |j\rangle\langle j|$ and $\hat{H}_I$ is the atom-light interaction Hamiltonian of the EIT medium given by form as

$$\begin{aligned}\hat{H}_I = \frac{\hbar}{2}\Big[&\left(\Omega^{+} e^{i(k_p z-\omega_p t)} + \Omega^{-} e^{i(-k_p z-\omega_p t)}\right)|3\rangle\langle 1| \\ &+\left(\Omega_c^{+} e^{i(k_c z-\omega_c t)} + \Omega_c^{-} e^{i(-k_c z-\omega_c t)}\right)|3\rangle\langle 2| + H.c.\Big].\end{aligned}$$

In equation (3), the operators accounting for the quasi 1D condensate dynamics take the form as $H_{sp} = -\frac{\hbar^2\partial_z^2}{2m} + \frac{1}{2}m\omega_z^2 z^2$, $H_{atom-light} = \frac{\hbar}{2}\left(\Omega^{+*}e^{-ik_p z} + \Omega^{-*}e^{ik_p z}\right)$ and $H_{int}^{j} = g_{jj}|\psi_l|^2 + g_{jl}|\psi_l|^2$ which are the single-particle, atom-light interaction, and nonlinear interaction Hamiltonians, respectively. The quasi 1D nonlnear interaction constant takes the form as $g_{jl} = \frac{2\pi a_{jl}\omega_r N_{bec}}{\omega_z a_{osc}}$ where $a_{osc} = \sqrt{\frac{\hbar}{m\omega_z}}$ is oscillator length. The ω_r and ω_z are the transverse and longitudinal trapping frequencies, respectively, where we use $(\omega_r, \omega_z) = 2\pi\times(100, 2.1\times 10^3)$ Hz in the simulation. The optical coherence of the condensate is given by $\sigma_{eg} = \psi_e\psi_g^*$. In the presence of circulating SR fields, the macroscopic wave functions and coherence would consist of high $\pm nk_p$ modes, i.e. $\psi_g = \sum_{n=-\infty}^{\infty}\psi_g^{(n)}e^{i(2n+1)k_p z}$, $\psi_e = \sum_{n=-\infty}^{\infty}\psi_e^{(n)}e^{i2nk_p z}$, and $\sigma_{eg} = \sum_{n=-\infty}^{\infty}\sigma_{eg}^{(n)}e^{ink_p z}$ with $\psi_{e,g}^{(n)}$ and $\sigma_{eg}^{(n)}$ being the spatially slowly-varying envelope. The coherence terms, $\sigma_{eg}^{(\pm 1)}$ carrying $e^{\pm ik_p z}$ account for the generation of SR fields.

The dynamics of the condensate flying through the cavity is simulated by the initial state where all the atoms are condensed in the excited state forming a Thomas-Fermi density profile while the ground state consists of quantum fluctuations sampled according to the truncated Wigner approximation of $\psi_g = \sqrt{1/N_{BEC}}\sum_{j=1}^{M}\alpha_j\xi_j(z)$, $<\alpha_j^*\alpha_l> = \delta_{jl}/2$, and $\xi_j(z)$ being an orthonormal basis.

Equations (1)-(4) are numerically solved by the method of lines where the Bloch and GP equations are propagated by the Fourier pseudospectral method and the adaptive Runge-Kutta method of orders 4 and 5 (RK45) for space and time integration, respectively, while the SR fields are integrated by the semi-Euler method. In the simulation, the total number of Fourier modes is 5×2^{12} and the number of mode for sampling initial fluctuations is $M = 3000$.

---

[1] X. Maître, E. Hagley, G. Nogues, C. Wunderlich, P. Goy, M. Brune, J. M. Raimond, and S. Haroche, Phys. Rev. Lett. **79**, 769 (1997).

[2] O. Kocharovskaya and Y. I. Khanin, Sov. Phys. JETP **63**, 945 (1986).

[3] K.-J. Boller, A. Imamoğlu, and S. E. Harris, Phys. Rev. Lett. **66**, 2593 (1991).

[4] W. Ketterle, Rev. Mod. Phys. **74**, 1131 (2002).

[5] F. Brennecke, T. Donner, S. Ritter, T. Bourdel, M. Köhl, and T. Esslinger, Nature **450**, 268 (2007).

[6] S. Inouye, A. Chikkatur, D. Stamper-Kurn, J. Stenger, D. Pritchard, and W. Ketterle, Science **285**, 571 (1999).

[7] P. Meystre, *Atom optics* (Springer Science & Business Media).

[8] I. D. Leroux, M. H. Schleier-Smith, and V. Vuletic, Phys. Rev. Lett. **104** (2010).

[9] L.-M. Duan, M. D. Lukin, J. I. Cirac, and P. Zoller, Nature **414** (2001).

[10] H. J. Kimble, Nature **453** (2008).

[11] T. Schumm, S. Hofferberth, L. M. Andersson, S. Wildermuth, S. Groth, I. Bar-Joseph, J. Schmiedmayer, and P. Krüger, Nature Physics **1**, 57 (2005).

[12] L. Dong, L. Zhou, B. Wu, B. Ramachandhran, and H. Pu, Phys. Rev. A **89**, 011602(R) (2014).

[13] M. Bajcsy, A. S. Zibrov, and M. D. Lukin, Nature **426**, 638 (2003).

[14] Y.-W. Lin, W.-T. Liao, T. Peters, H.-C. Chou, J.-S. Wang, H.-W. Cho, P.-C. Kuan, and I. A. Yu, Phys. Rev. Lett. **102**, 213601 (2009).

[15] F. Haake, H. King, G. Schröder, J. Haus, and R. Glauber, Phys. Rev. A **20**, 2047 (1979).

[16] M. Gross and S. Haroche, Physics Reports **93**, 301 (1982).

[17] T. Peters, S.-W. Su, Y.-H. Chen, J.-S. Wang, S.-C. Gou, and I. A. Yu, Phys. Rev. A **85**, 023838 (2012).

[18] D. E. Chang, L. Jiang, A. Gorshkov, and H. Kimble, New Journal of Physics **14**, 063003 (2012).

[19] N. S. Ginsberg, S. R. Garner, and L. V. Hau, Nature **445**, 623 (2007).

[20] J. M. Zhang, F. C. Cui, D. L. Zhou, and W. M. Liu, Phys. Rev. A **79**, 033401 (2009).

[21] P. B. Blakie, A. S. Bradley, M. J. Davis, R. J. Ballagh, and C. W. Gardiner, Adv. Phys. **57**, 353 (2008).

[22] D. Stadler, S. Krinner, J. Meineke, J.-P. Brantut, and T. Esslinger, Nature **491**, 736 (2012).

[23] P. M. Duarte, R. A. Hart, J. M. Hitchcock, T. A. Corcovilos,

T.-L. Yang, A. Reed, and R. G. Hulet, Phys. Rev. A **84**, 061406 (2011).
[24] Y.-F. Hsiao, H.-S. Chen, P.-J. Tsai, and Y.-C. Chen, Phys. Rev. A **90**, 055401 (2014).
[25] F. Blatt, T. Halfmann, and T. Peters, Opt. Lett. **39**, 446 (2014).
[26] C. H. Keitel, M. O. Scully, and G. Süssmann, Phys. Rev. A **45**, 3242 (1992).
[27] N. Rohringer, D. Ryan, R. London, M. Purvis, F. Albert, J. Dunn, J. Bozek, C. Bostedt, A. Graf, R. Hill, *et al.*, Nature **481**, 488 (2012).
[28] S. M. Cavaletto, Z. Harman, C. Ott, C. Buth, T. Pfeifer, and C. H. Keitel, Nature Photonics **8**, 520 (2014).
[29] D.-W. Wang, S.-Y. Zhu, J. Evers, and M. O. Scully, Phys. Rev. A **91**, 011801 (2015).

Supplemental Materials: All-optical control of superradiance and matter waves using a dispersive cavity

Shih-Wei Su, Zhen-Kai Lu, Nina Rohringer, Shih-Chuan Gou and Wen-Te Liao

(Dated: July 22, 2017)

In this supplementary material, we present the equation of motion and the condensate dynamics in more detail.

In the presence of counter-propagating coupling fields $\Omega_c^\pm$ and the superradiant fields $\Omega^\pm$, the dynamics of the EIT mirror is described by the optical-Bloch equation which reads:

$$\partial_t\rho_{12} = -i\left(\Delta-\Delta_c\right)\rho_{12} - i(\Omega_c^+\rho_{13}^+ + \Omega_c^-\rho_{13}^-)/2 + i(\Omega^{+*}\rho_{32}^+ + \Omega^{-*}\rho_{32}^-)/2, \tag{S1}$$

$$\partial_t\rho_{13}^\pm = -\left(i\Delta+\Gamma/2\right)\rho_{13}^\pm - i\Omega_c^{\pm*}\rho_{12}/2 - i\Omega^{\pm*}\left(\rho_{11}-\rho_{33}\right)/2, \tag{S2}$$

$$\partial_t\rho_{23}^\pm = -\left(i\Delta_c+\Gamma/2\right)\rho_{23}^\pm - i\Omega^{\pm*}\rho_{21} + i\Omega_c^{\pm*}\left(\rho_{33}-\rho_{22}\right), \tag{S3}$$

$$\partial_t\rho_{11} = \Gamma\rho_{33}/2 + Im\left[\Omega^+\rho_{13}^+ + \Omega^-\rho_{13}^-\right], \tag{S4}$$

$$\partial_t\rho_{22} = \Gamma\rho_{33}/2 + Im\left[\Omega_c^+\rho_{23}^+ + \Omega_c^-\rho_{23}^-\right], \tag{S5}$$

$$\partial_t\rho_{33} = -\Gamma\rho_{33} - Im\left[\Omega^+\rho_{13}^+ + \Omega^-\rho_{13}^- + \Omega_c^+\rho_{23}^+ + \Omega_c^-\rho_{23}^-\right], \tag{S6}$$

where Γ is the spontaneous decay rate of the excited state $|3\rangle$ and ρ_{ij} is the element of the density matrix. In equations (S1)-(S6), all fast-oscillation exponential factors associating with center frequencies and wave factors have been eliminated, and only slowly-varying profiles are retained.

When the condensate is loaded in the dispersive cavity, in the presence of the interaction between the circulating SR fields and condensate, the ground-state and excited condensate wave functions constitute the superposition of discrete $\pm(2n+1)k_p$ and $\pm 2nk_p$ plane waves, respectively. In this manner the condensate wave function can be decomposed as :

$$\psi_g = \sum_{n=-\infty}^{\infty}\psi_g^{(n)}e^{i(2n+1)k_pz}, \tag{S7}$$

and

$$\psi_e = \sum_{n=-\infty}^{\infty}\psi_e^{(n)}e^{i2nk_pz},$$

where $\psi_{e,g}^{(n)}$ are slowly-varying profiles. As depicted in Fig. S1 **a** and **b**, the momentum-space density profile of single realization of $d^{opt} = 500$ and $\Omega_c = 2\Gamma$ shows the clear generation of these discrete $\pm nk_p$ modes. Furthermore the Fourier transform of the coherence σ_{eg} depicted in Fig. S1 **c** shows clear superposition of $\pm nk_p$ modes.

The coherent SR-BEC interaction transfer most of the atoms to the ground state while the rest of them decay to other states due to the incoherent spontaneous processes as shown in Fig. S1 **d**. Therefore the dynamics of the condensate after passing through the cavity is described by the single component Gross-Pitaevskii equation which reads

$$i\hbar\partial_t\psi_g = \left(-\frac{\hbar^2}{2m}\partial_z^2 + \frac{m\omega_z^2z^2}{2} + g_{gg}\left|\psi_g\right|^2\right)\psi_g, \tag{S8}$$

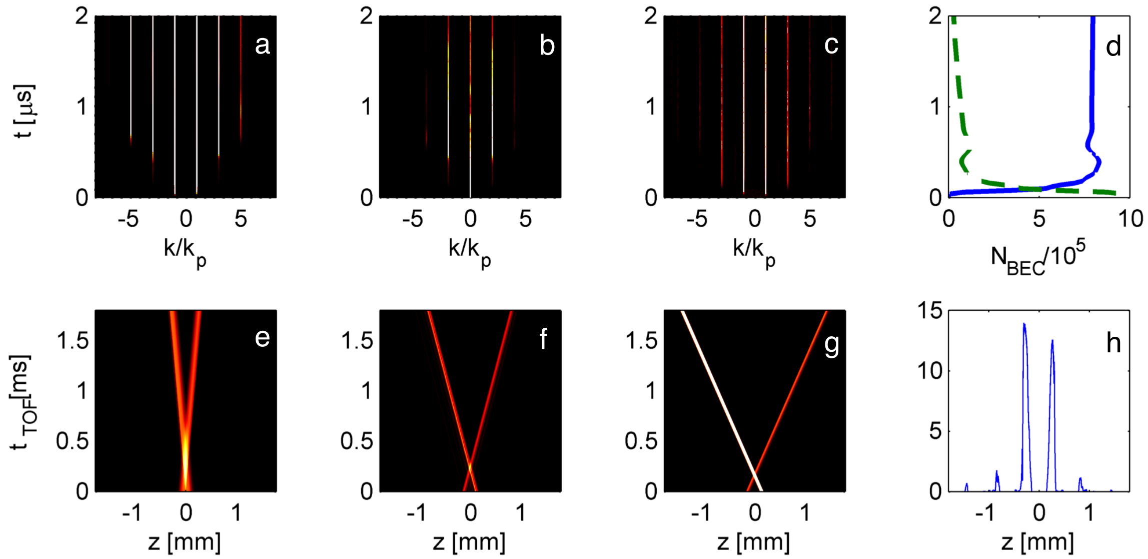

FIG. S1. Panels **a**-**d** show the dynamics of the binary BEC inside the EIT cavity of $d^{opt} = 500$ and $\Omega_c = 2\Gamma$ within 2 μs. The evolution of the condensate densities in momentum space are shown in panels **a** and **b** where the high odd k_p modes are generated in ψ_g while the even k_p modes are generated in ψ_e. Panel **c** shows the optical coherence σ_{eg}. The coherent transfer of the BEC particle number from states $|e\rangle$ (green dashed-dotted line) to $|g\rangle$ (blue solid line) is shown. Panels **e**-**h** represent the time-of-fight simulation after the condensate is released from the cavity and harmonic trap. Panels **e**-**g** are the density components carry the momenta $\pm k_p$, $\pm 3k_p$, and $\pm 5k_p$, respectively. The total density profile $|\psi_g|^2$ at $t_{TOF} = 1.8$ ms. The contrast of the 2D plots is adjusted for better visualization.

where we neglect the cross-species and atom-light interactions.

During the time of flight (TOF) measurement, the condensate would split into several atomic clouds which corresponds to different $\pm nk_p$ modes. To simulate the TOF dynamics, we numerically integrated equation. S8 by removing the trapping potential and interactions. As shown in Fig. S1 **e**-**h**, we perform the TOF simulation for $\Delta t_{TOF} = 1.8$ ms. In Fig. S1 **e**-**g**, the evolution of the condensed atoms carrying momenta are plotted and the velocities can be calculated from the slopes which agrees with the expected values, $\pm\hbar k_p/m$, $\pm 3\hbar k_p/m$, and $\pm\hbar k_p/m$. In Fig. S1 **h**, the total density distribution at $t_{TOF} = 1.8$ ms is shown where six density bumps that are symmetric to the origin can be clearly observed. The two innermost density bump pair in Fig. S1 **h** corresponds to the $\pm k_p$ modes while the density bump pair located around $z = \pm 0.5$ mm is the $\pm 3k_p$ modes and the outermost pair carries $\pm 5k_p$ momenta.